

Use of fluid dynamics computational to investigate heat exchanges in plate systems solar floating

Hicaro RD Silva ¹, Camila O. dos S. Borges ², Nuccia CA Sousa ¹

¹Department of Production Engineering, Federal University of Alagoas
Beira Rio Avenue, 57200-000, Penedo /Alagoas, Brazil.

hicaro.dionizio@arapiraca.ufal.br, nuccia.sousa@penedo.ufal.br

²Engineering Department Mechanics, Federal University of Western Bahia
Dr. Manoel Avenue Novaes, 47600-000, Bom Jesus da Lapa/Bahia, Brazil.
camila.b2190@ufob.edu.br

Abstract. The module efficiency photovoltaic is influenced by temperature and incident solar radiation. Thus, the analysis thermal panels solar is crucial, considering the growing demand for energy and its feasibility economic. In this research, we use computational tools to analyze the performance thermal panels solar installed in means with different temperatures, considering a model with the plate installed over water and another with just air flow below, with the aim of comparing the two settings. The study he was accomplished using Fluid Dynamics Computational (CFD) in free software OpenFOAM, Salome-Meca and Paraview. We obtained you temperature gradients of each of the models simulated, having as main result a difference of approximately 5 K (5 °C) between the floating solar panel (installed over the water) and not floating, beyond the behavior thermal to the over the simulation time steps in the two situations.

Keywords: Solar panels; Computational fluid dynamics; OpenFOAM.

1 Introduction

For Villalva and Gazoli [1], solar radiation, in the context of energy generation, is a clean and renewable form of transformation that has been widely used in recent times. The light energy of the sun can be converted directly into electricity through the photovoltaic effect. This process occurs in photovoltaic cells, which can be built using different technologies, such as thin-film crystalline silicon.

Izadian et al. [2] mentioned in their work that the current in a photovoltaic panel has a behavior similar to a diode and can be represented by Equation (1).

$$I_D = I_{Sat} \left[e^{\frac{q}{nkT_c}} - 1 \right] \quad (1)$$

Where I_{Sat} is the reverse saturation current, q is the charge of the electron, n is the ideality factor of the diode, k is the Boltzmann constant and T_c is the cell temperature on an absolute scale, and is therefore the factor that influences the efficiency of the photovoltaic panel, since the temperature of the photovoltaic cell reaches values above the ambient temperature. This fact directly affects the temperature of a solar panel, since solar panels are tested at 25°C (77°F) in standard test conditions (STC), according to the website Energia Solar Shop [3]. However, in some regions of the planet, solar panels can reach higher temperatures during operation, which can affect their efficiency and performance.

In their research, Santafé et al. [4] mentioned that reducing evaporation levels in reservoirs, combined with

reducing the average temperature of the panels, presents advantages from an economic point of view. In irrigation reservoirs in arid and semi-arid areas, surface evaporation can be reduced.

Based on Ilgen et al. [5], it can be said that there are few studies that sufficiently describe the impact of a floating solar plant on the temperature of the environment and water. Given this need, in this work we seek to investigate the distribution of temperatures in the two installation media in which the panel can be inserted, performing this thermal analysis through Computational Fluid Dynamics (CFD). Through the use of CFD with free and open-source tools, the thermal behavior of a solar module installed on water will be acquired, and for comparison, the behavior of the same module containing only air below.

2 Methodology

The CFD model building process is generally divided into three essential steps: Pre-processing, Processing and Post-processing. Each step can use different programs, which can be free or paid. In this work, only free software was used: Salome-Meca [6] for pre-processing, OpenFOAM [7] for processing and ParaView [8] for post-processing.

Initially, in pre-processing via Salome -Meca, modeling is performed by creating the geometry, known as CAD (Computer Aided Design). It generates the computational domain of the simulation, including desired measurements and structures. The mesh is then created from this geometry, dividing it into small pieces through a process called mesh discretization .

The processing then uses the mesh to perform simulation calculations. The OpenFOAM software solves the equations of interest by the of Finite Volumes using the buoyantSimpleFoam solver, which employs the k- Epsilon turbulence model , containing the following equations:

The transport equation for turbulent kinetic energy (k), represented by Equation (2).

$$\frac{\partial(\rho k)}{\partial t} + \frac{\partial(\rho k u_i)}{\partial x_i} = \frac{\partial}{\partial x_j} \left[\left(\mu + \frac{\mu_t}{\sigma_k} \right) \frac{\partial k}{\partial x_j} \right] + P_k - \rho \varepsilon \quad (2)$$

Transport equation for the dissipation rate (ε), represented by Equation (3).

$$\frac{\partial(\rho \varepsilon)}{\partial t} + \frac{\partial(\rho \varepsilon u_i)}{\partial x_i} = \frac{\partial}{\partial x_j} \left[\left(\mu + \frac{\mu_t}{\sigma_\varepsilon} \right) \frac{\partial \varepsilon}{\partial x_j} \right] + C_{1\varepsilon} \frac{\varepsilon}{k} P_k - C_{2\varepsilon} \rho \frac{\varepsilon^2}{k} \quad (3)$$

Furthermore, the fundamental physical principles resolved by the solver are those of conservation of mass, momentum and energy, expressed below in tensor form to maintain the generality and three-dimensional accuracy of the simulation.

Conservation of mass is represented by Equation (4).

$$\frac{\partial \rho}{\partial t} + \frac{\partial(\rho u_i)}{\partial x_i} = 0 \quad (4)$$

Conservation of momentum through the Navier-Stokes Equation, represented by equation (5).

$$\frac{\partial(\rho u_i)}{\partial t} + \frac{\partial(\rho u_i u_j)}{\partial x_j} = - \frac{\partial p}{\partial x_i} + \frac{\partial \tau_{ij}}{\partial x_j} + \rho g_i \quad (5)$$

And the conservation of energy considering thermal conduction and viscous work, represented by Equation (6).

$$\frac{\partial(\rho E)}{\partial t} + \frac{\partial(\rho u_i H)}{\partial x_i} = - \frac{\partial}{\partial x_i} \left(k \frac{\partial T}{\partial x_i} \right) + \frac{\partial}{\partial x_i} (u_i \tau_{ij}) \quad (6)$$

Definition of the variables of equations (2), (3), (4), (5) and (6): ρ is the fluid density; μ_t is the turbulent viscosity; k is the turbulent kinetic energy per unit mass; σ_k is the turbulent Prandtl number for k (model constant); P_k is the production of turbulent kinetic energy; ε is the rate of dissipation of turbulent kinetic energy; σ_ε is the Prandtl turbulent number for ε (model constant); $C_{1\varepsilon}$ and $C_{2\varepsilon}$ are empirical model constants; u_i is the time component of the fluid velocity for the x , y , and z directions respectively; x_i is a spatial coordinate in the direction i ; p is the pressure; τ_{ij} is the viscous stress tensor; g_i is the component of the gravitational acceleration in the direction i ; E is the total energy per unit volume; H is the total enthalpy per unit mass; T is the temperature and $u_i \tau_{ij}$ is the work done by the viscous forces.

These equations are fundamental to the standard 3D fluid dynamics modeling of OpenFOAM and were used in this case. They are provided by the official solver documentation, available and explained on the OpenFOAM website .

Furthermore, two essential configurations in the processing step are the fvSchemes and fvSolution files . fvSchemes defines how the partial differential equations are discretized , determining the numerical method for the spatial and temporal derivative of the equations. fvSolution specifies the numerical solution parameters, such as the pressure correction schemes and the solution algorithms used to solve the fluid dynamics equations.

fvSchemes file , the settings have been applied for a steady-state resolution , meaning that there is no variation in time, where the Gaussian method with linear interpolation is being used to calculate the gradients without applying any standard scheme for divergences that are not explicitly defined. In addition, the Gaussian method with linear interpolation and correction for the Laplacian calculation and a correction scheme for the normal gradient are being used, both improving the accuracy aspects of the non-orthogonal parts of the mesh.

In fvSolutions it was configured so that the p_{rgh} (relative pressure corrected by the hydrostatic component of the flow) uses the incomplete diagonal preconditioning solver cholesky with absolute tolerance at 1×10^{-8} and relative tolerance at 0.01; For the criteria of the variables the $(U | e | k | epsilon)$ PBiCGStab solver is used , which is the method of preconditioned stabilized biconjugate gradients and relative tolerance at 0.01; in addition, the algorithm is used *SIMPLE*(Semi-implicit Method Pressure-Linked Equation) which is the iterative method used to solve the coupled Navier -Stokes equations in steady state, applying the number of non-orthogonal corrections and the pressure references in a specific cell with a value equal to 0. Finally, the limit of residuals of p_{rgh} and e in 1×10^{-2} and for U in 1×10^{-4} . It is worth remembering that U is the fluid flow velocity, e is the internal energy and k is the turbulent kinetic energy, already mentioned previously.

The boundary conditions used to perform the simulation are shown in Tables 1, which represents the simulation of the non-floating plate, and in Table 2, which represents the boundary conditions of the simulation of the floating solar plate (above the water).

Table 1 – Contour conditions for the simulation of the non- floating solar panel

Boundary conditions	Value
Air inlet speed	1.8 m/s
Inlet temperature of the fluid	298.15K
Air inlet temperature	353.15K
Pressure hydrostatic in the entire control volume	0 Pa
Pressure absolute in the entire control volume	101320 Pa

Table 2 – Contour conditions for the floating solar panel simulation

Boundary conditions	Value
Air inlet speed	1.8 m/s
Ground speed (Water)	0.1 m/s
Air inlet temperature	298.15K
Solar panel temperature	353.15K
Soil (water) temperature	293.15K
Pressure hydrostatic in the entire control volume	0 Pa
Pressure absolute in the entire control volume	101320 Pa

In the next section, the results of the post-processing will be presented , where the power of the free software ParaView can be highlighted , which was responsible for aggregating, selecting and converting the numerical data from the processing into easy-to-understand visual information.

3 Results and Discussions

For this simulation, two computational domains were designed, both with the same dimensions and containing a solar panel installed in the center at an inclination angle of 15° , very similar to how it would be

installed in the real world, as exemplified in Figure 1.

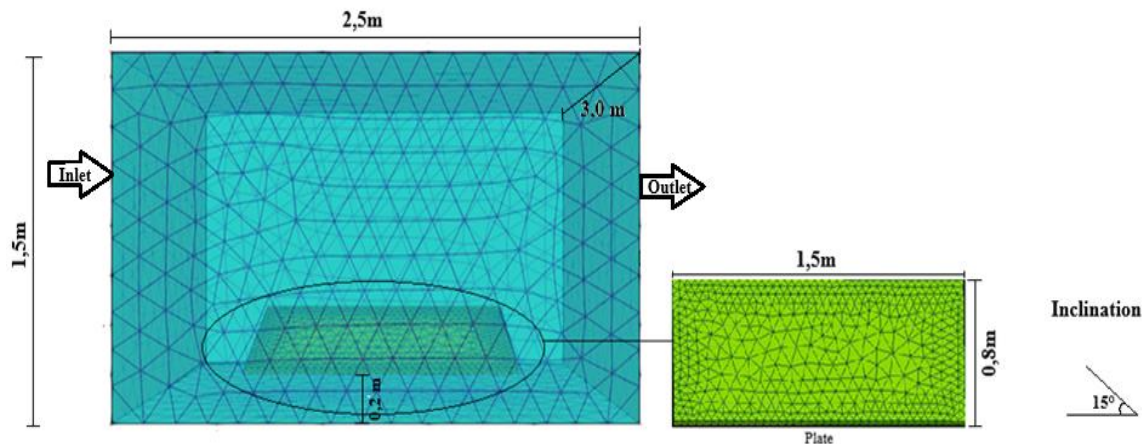


Figure 1: Full discretized mesh of the case geometry and its physical representation

With the mesh ready, converted and exported from the “.HDF ” extension to “.UNV” in OpenFOAM , the software can be asked to analyze the structure of this mesh before starting the simulation, allowing problems to be identified in advance.

Table 1 contains the parameters described by the analysis of the OpenFOAM mesh verification itself . All mesh quality criteria are met without significant problems for the results, indicating that the discretization of the computational domain is ready to be used in the simulation and that the probability of numerical problems related to the mesh is minimal. We also highlight that there is a wide range of possibilities for studies related to mesh refinement for computational simulations.

Table 3 – CheckMesh made by OpenFOAM

Classes	Parameters	Definition
Mesh Statistics	Points	7722
	Total faces	80753
	Internal faces	76663
	Cells	39354
	Faces per cell	4
Cell Types	Tetrahedral	39354
Checking the general topology of the mesh	Definition of neighborhood	OK
	Cell addressing	OK
	Triangular ordering	OK
	Face vertices	OK
	Regions	OK
Checking the topology of connected cells	Plate region	OK
	Water region	OK
	Atmosphere region	OK
Mesh check final result		Mesh Ok

3.1 Plate installed about the air

Based on the boundary conditions in Table 1, the simulation was set to a time step of 2,000 to confirm the convergence of the results, since the solver is stationary. The results of all time steps were not saved due to the

high computational cost and the similarity between consecutive steps. Only the data from every 50 steps were saved, as exemplified in Figure 2.

For more accurate results in this study, a point directly below the plate was chosen, and temperatures were observed at three different heights: 0.05 m, 0.1 m, and 0.15 m. All these distances are measured from the surface where the plate is installed, with the height of 0.15 m being the closest to the space where the PV module is located. Figure 3 represents the temperature measurements at this stage.

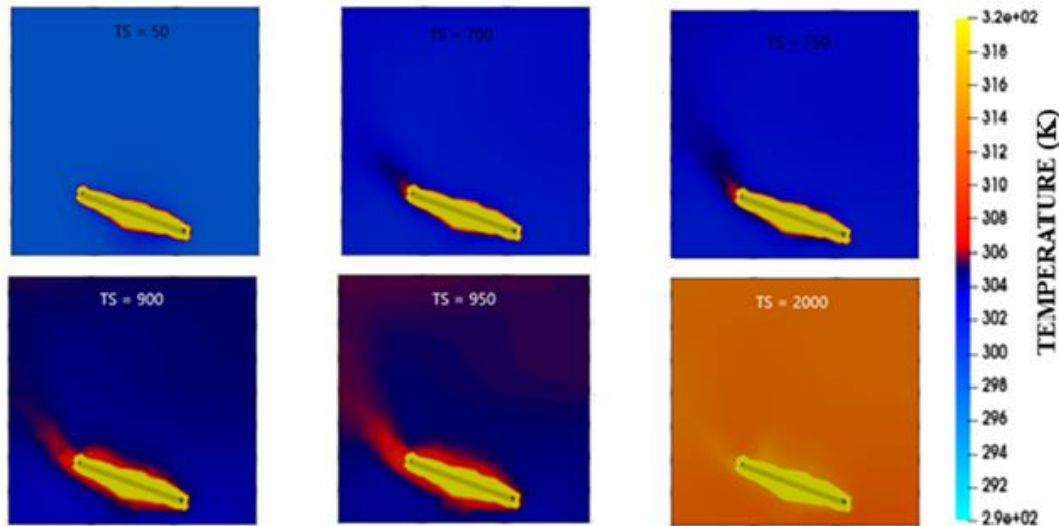


Figure 2: Thermal behavior of the plate on air at various time intervals (TS)

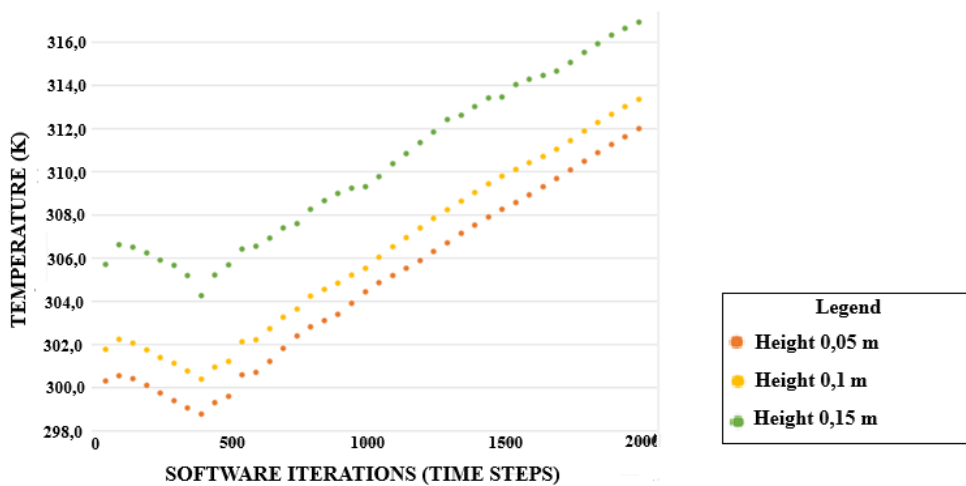


Figure 3: Temperatures measuring heights from the ground to the plate above the air

3.2 Plate installed over the water

In Table 2, the configuration of this case differs from the previous one due to the information additional on speed and temperature in the soil boundary, which will be considered the water below the plate. Therefore, it is estimated that the water moves at a constant rate of 0.1 m/s and a temperature of 293.15 K (20° C). In the same way as the previous one, this simulation was also configured in the same solver already mentioned and in 2000 time steps, saving the results every 50 time steps, exemplified in Figure 4.

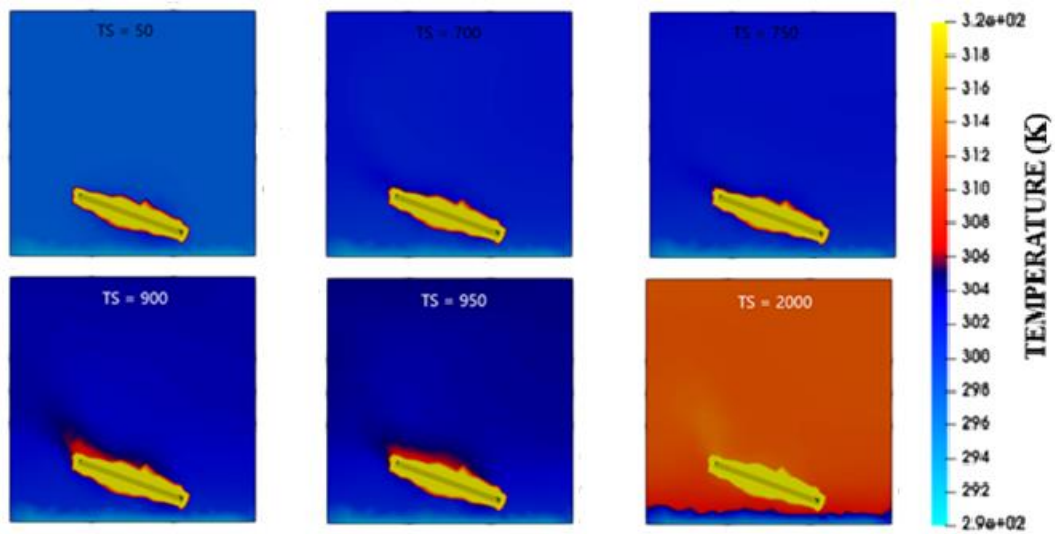


Figure 4 - Thermal behavior of the plate on water at different time intervals (TS)

As in the previous simulation, central points were chosen at the same heights of 0.05 m, 0.10 m and 0.15 m. With the data from Figure 5 on temperature as a function of time steps, it will be possible to observe the difference between the two situations more visibly, facilitating a possible decision regarding a better grouping of the photovoltaic systems.

However, in this simulation, water temperature measurements were also taken during the interactions to better understand what happens as the program calculates the interactions. Figure 6 shows the behavior of the water temperature over the time steps.

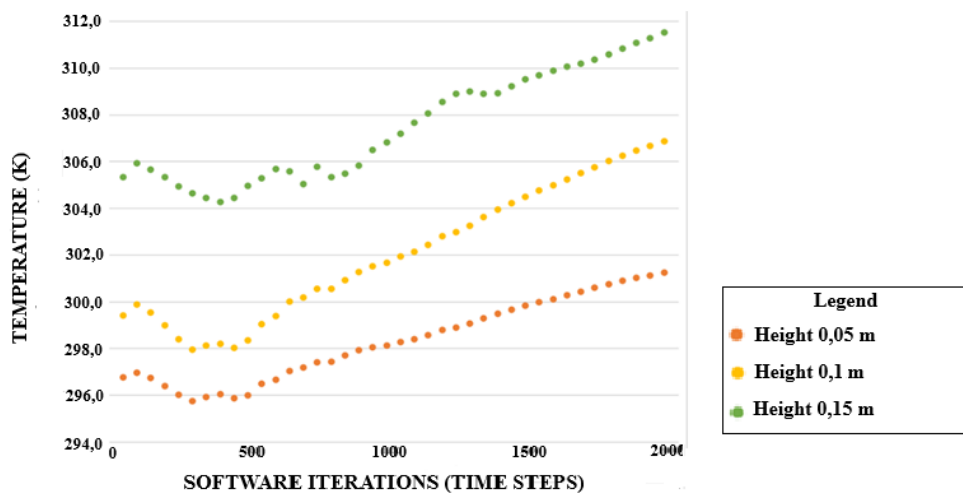


Figure 5 – Temperatures measuring heights from the water to the floating plate

Figure 5 shows a reduction in the final temperature near the plate, regardless of the measurement height. Compared to the plate installed in air, there is a difference of approximately 5 K at the same measurement points, which would directly affect the final operating temperature of the plate, given the search for thermal equilibrium between the environment and the object.

However, as noted earlier, there was also concern about what would happen to the temperature of the water below the plate. Figure 6 shows the water temperature curve with a slight slope, going from its initial temperature of 293.15 K to 294.77 K at the end of the last time step of the simulation.

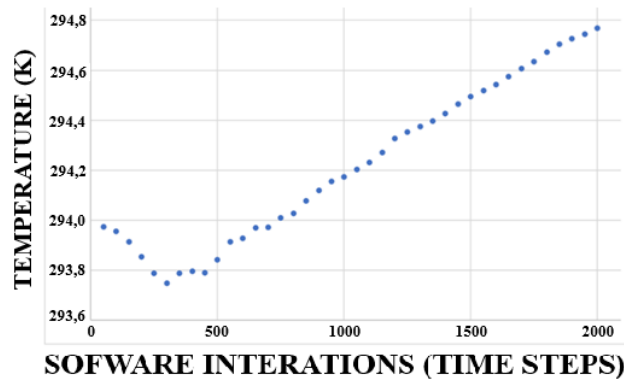


Figure 6 – Water temperature during simulation

4 Conclusions

Firstly, throughout this work, it was possible to glimpse how free tools, specifically the open source software OpenFOAM, can comprehensively represent the results of the case simulation. Therefore, the dissemination of these tools is of extreme importance to increase visibility in the Brazilian national territory, allowing any researcher interested in bringing innovations to all areas of engineering and physics to explore them.

Furthermore, the temperature difference observed between the plate installed above the water and the air is approximately 5 K, corroborating the efficiency increase factor. However, based on Figure 6, the water temperature had a difference of more than 1.5 K, which may become a cause for concern.

This temperature difference found by the simulation performed is close to the temperature difference found in the real experiments of the works of Ilgen et al. [5] and Alencar Filho et al. [9], performed under conditions similar to those simulated. These similar results demonstrate that CFD is an excellent path to be taken based on its accuracy and argue that the mesh used in this case is in accordance with the expected standards, combining a good computational cost with the accuracy of the results.

Finally, based on all the data presented, in order to guarantee life in the water of the reservoir, a more in-depth study of the effects of this increase in temperature is necessary, given the sensitivity of that medium. However, it is clear that, from an economic point of view, the installation of floating solar modules is remarkably efficient. This configuration would reduce water evaporation, increase the efficiency of the panels, utilize the space above the water and use the water from the reservoir itself to clean the solar modules.

References

- [1] VILLALVA, MG; GAZOLI, JR Photovoltaic Solar Energy: Concepts and Applications. Editora Érica, 2014.
- [2] Izadian, Afshin & Pourtaherian, Arash & Motahari, Sarasadat. (2012). Basic model and governing equation of solar cells used in power and control applications.
- [3] How does temperature affect solar panel efficiency? Solar Energy Store, 2021.
- [4] Ferrer Gisbert, CM.; Ferran Gozálviz, JJ.; Redón Santafé, M.; Ferrer- Gisbert, P.; Sánchez Romero, F.; Torregrosa Soler, JB. (2013). A new floating roof photovoltaic system for water reservoirs. *Renewable energy*. (60):63-70.
- [5] Ilgen, K., Schindler, D., Wieland, S., & Lange, J. (2023). The impact of floating photovoltaic power plants on lake water temperature and stratification. *Scientific Reports*, 13 (1), 7932.
- [6] SimulEase, Code_Aster for Windows, Salome_Meca, 2021. Available at: <https://code-asterwindows.com/>.
- [7] The OpenFOAM Foundation, OpenFOAM 2023. Available at: <https://openfoam.org/>.
- [8] ParaView, ParaView 2023. Available at: <https://www.paraview.org/>.
- [9] Alencar Filho, AARD, Carvalho, PCMD, & Dupont, IM (2018). Influence of the distance of photovoltaic panels in relation to water on energy efficiency.

Declaration of authorship

The authors confirm that they are solely responsible for the authorship of this work and that all material included here as part of this work is the property (and authorship) of the authors or has the permission of the owners to be included here.